The mechanism and effect of defects in the B1–B2 phase transition of KCl under high pressure: molecular dynamics simulation

2005 J. Phys.: Condens. Matter 17 1027

(http://iopscience.iop.org/0953-8984/17/6/021)

INSTITUTE OF PHYSICS PUBLISHING JOURNAL OF PHYSICS: CONDENSED MATTER

J. Phys.: Condens. Matter **17** (2005) 1027–1035 doi:10.1088/0953-8984/17/6/021

The mechanism and effect of defects in the B1–B2 phase transition of KCl under high pressure: molecular dynamics simulation

Takahiro Kinoshita[1], **Tsutomu Mashimo**[1,3] **and Katsuyuki Kawamura**[2]

[1] Shock Wave and Condensed Matter Research Centre, Kumamoto University, 2-39-1 Kumamoto 860-8555, Japan
[2] Department of Earth and Planetary Sciences, Tokyo Institute of Technology, 2-12-1 Ookayama, Meguro-ku, Tokyo 152-8551, Japan

E-mail: mashimo@gpo.kumamoto-u.ac.jp

Received 2 August 2004, in final form 4 January 2005
Published 28 January 2005
Online at stacks.iop.org/JPhysCM/17/1027

Abstract

Molecular dynamics (MD) simulations of the pressure-induced phase transition of potassium chloride (KCl) were performed with 2744 and 9000 atoms to study crystalline states, the process and the effects of defects under high hydrostatic pressure. In this study, we adopted the Born–Mayer–Huggins-type potential function to describe the interatomic interaction. The potential parameters used in this study were empirically optimized on the basis of Hugoniot equation of state data. The simulation results for perfect crystals (1372 K^+ and 1372 Cl^-) showed that the B1–B2 phase transition occurred with large hysteresis, and the thermodynamic transition pressure was calculated to be 3.5 GPa. The simulation results indicated that the phase transition proceeded through displacements of atomic lines parallel to the ⟨100⟩ axis direction of the B1-type structure, and that these lines corresponded to the atomic lines parallel to the ⟨111⟩ axis direction of the B2-type structure after the phase transition. In the case of the larger cells containing 9000 atoms with weak or strong van der Waals interactions, some clusters or dislocations, respectively, were generated in the resultant B2 phase. As regards dislocations, the phase transitions started around dislocations and the phase transition pressure decreased.

(Some figures in this article are in colour only in the electronic version)

1. Introduction

Potassium chloride (KCl) is a typical ionic crystal with a NaCl (B1) type of structure under ambient conditions, and transforms to a CsCl (B2) type of structure under high pressure. The

[3] Author to whom any correspondence should be addressed.

phase transition and equation of state (EOS) of KCl have been investigated under hydrostatic and shock compressions, and the B1–B2 phase transition pressures of KCl are reported to be around 2 GPa [1–6].

In studies done under static compression, Bridgman first determined the compression curves and found that the phase transition of KCl occurred at 1.97 GPa [1]. Bassett *et al* determined the volume change of KCl to be 0.11 ± 0.005, and found it associated with the B1–B2 phase transition at room temperature using x-ray diffraction employing a DAC [2]. In studies done under shock compression, Hayes measured the stress hysteresis of $\langle 100 \rangle$ and $\langle 111 \rangle$ directions with quartz stress gauges, and reported that the phase transition occurred at about 2 GPa [7]. Dremin *et al* observed the phase transition at 1.89 GPa using an electromagnetic gauge method [8]. Mashimo *et al* found that the phase transitions along the $\langle 100 \rangle$, $\langle 110 \rangle$ and $\langle 111 \rangle$ axis directions occurred at 2.5, 2.2 and 2.1 GPa, respectively, by inclined-mirror and VISAR methods [9].

It has been pointed out that the presence of impurities generally reduces hysteresis, and that defects in the form of vacancies, grain boundaries and dislocations act as 'triggers' for the phase transition [10]. However, the process of the phase transition and the effects of defects have not been fully observed. Observing the process of phase transitions under high pressure is very difficult, because phase transitions finish within ps or ns orders. We discuss the process of phase transitions and the effects of defects in such short time phenomena using molecular dynamics (MD) simulation.

Many MD simulation studies on molten and aqueous solutions etc have been reported for KCl, but there have been only a few reports on the polymorphic phase transitions of solid KCl. Parrinello *et al* carried out a constant pressure molecular dynamics simulation to study the B1–B2 phase transition in KCl, reporting that B1-type structures transformed to B2-type structures throughout the metastable rock-salt state in the process of increasing pressure [11]. Their results indicated that a phase transition occurred by the displacement of particles, and this was different from Buerger's mechanism [12]. Ruff *et al* performed isothermal–isobaric molecular dynamics simulations of some alkali halides [13], and reported a polymorphic phase transition and variations of the pair correlation functions in the course of the phase transition; also confirming the Watanabe–Tokonami–Morimoto (WTM) mechanism [14] from the arrangements of atoms of the resultant B2 phase. Devani and Anwar investigated the effects of vacancies on the B1–B2 phase transition pressure, and reported that the phase transition was initiated at a defect site, and the B2 phase spread throughout the entire crystal [10]. The B1–B2 phase transition pressure and the hysteresis decreased as the number of vacancies increased. However, the numbers of atoms (256 K^+ and 256 Cl^-) in their simulations were too small for discussing crystalline states and the mechanism of the phase transition of KCl. Recio *et al* investigated the B1–B2 phase transition of alkali chlorides with *ab initio* calculations, and reported cohesive properties (lattice constants, lattice energies and bulk moduli) and phase transition pressures [15]. Their results agreed well with the experiments. It was, however, difficult to carry out large scale calculations by means of *ab initio* calculations, or to discuss the process of phase transitions, crystalline states and the effects of defects.

In this study, we carried out MD simulations for the B1–B2 phase transition of KCl as a basis for discussing the process and the effects of defects in the form of dislocations on phase transitions under high pressure. Calculations for larger cells were carried out to underpin discussions of the crystalline states. We also changed the potential parameters to allow discussion of the effects of van der Waals forces on the crystalline state of the resultant B2 phase.

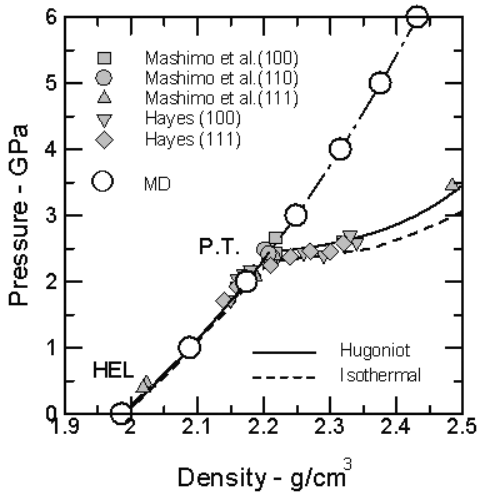

Figure 1. The Hugoniot compression curve, isothermal compression curve and MD simulation results in the low pressure region.

Table 1. Potential parameters used in this study and bulk moduli of KCl.

	Potential parameters			Bulk moduli of KCl		
	A	*B*	*C*		Hugoniot data	MD simulation
Cl	1.950	0.180	33.00	K_0 (GPa)	17.2	17.8
K	1.908	0.131	15.00	K_0'	4.9	5.1
				K_0'' (GPa^{-1})	−0.3	−0.3

2. Simulation method

We used the Born–Mayer–Huggins-type interatomic potential function, composed of a Coulombic attraction term, an exponential repulsion term and a van der Waals interaction term, which is due to polarization of molecules:

$$\phi(r_{ij}) = \frac{q_i q_j}{r_{ij}} + f(B_i + B_j)\exp\left[\frac{A_i + A_j - r_{ij}}{B_i + B_j}\right] - \frac{C_i C_j}{r_{ij}^6} \tag{1}$$

where r_{ij} is the interatomic distance between the ith and jth ion, and f is a standard force constant, 4.184 kJ Å^{-1} mol^{-1}. The effective charge q, the repulsive radius A, the softness parameter B and the van der Waals coefficient C are the potential parameters. These parameters were empirically optimized to reproduce lattice parameters and bulk moduli of KCl on the basis of the Hugoniot data [9]. The Hugoniot compression curve, isothermal compression curve and the MD results with pressure ranges up to 6 GPa are summarized in figure 1. Bulk moduli were evaluated by the method of least squares fitting to the Birch–Murnaghan equation of states. The bulk moduli and potential parameters used in this study are listed in table 1.

MD simulations were carried out using the simulation program 'MXDORTO' developed by Kawamura [16] in an isothermal–isobaric (NTP) condition to investigate the pressure-induced phase transition. Scaling algorithms of particle velocities and basic cell parameters were adopted to retain constant temperature T and pressure P, respectively. Desired pressures and temperatures were not suddenly required starting from another condition; we

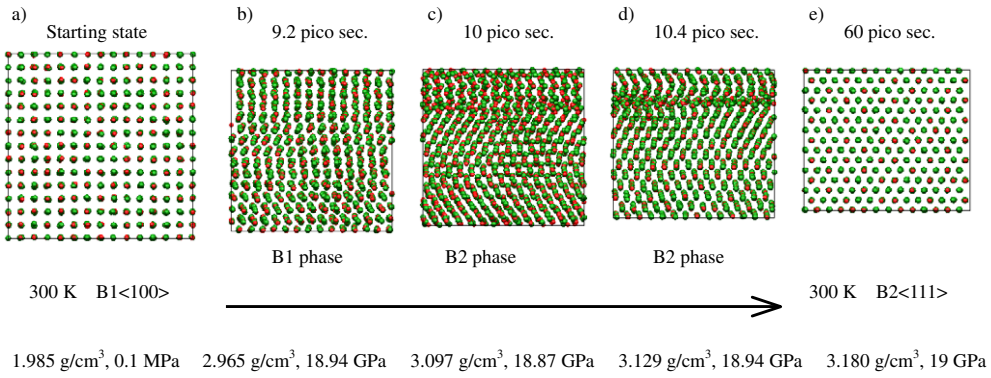

Figure 2. The process of the B1–B2 phase transition of KCl with a perfect crystal (1372 K^+ and 1372 Cl^-). The phase transition progressed to the arrow. Atomic lines along the ⟨100⟩ axis direction of a B1-type structure correspond to the ⟨111⟩ axis direction of a B2-type one.

increased pressure and temperature in every simulation step of two femtoseconds, and they converged to the desired value within several picoseconds. We imposed three-dimensional periodic boundary conditions and used the Ewald sum method [17] to efficiently converge the calculations of the Coulomb and the dispersion interaction. Newton's equation of motion was integrated numerically using the Verlet algorithm, setting the time interval at 2.0 fs.

2.1. Perfect crystal

A basic MD cell with 343 unit cells ($7 \times 7 \times 7$), containing 2744 atoms (1372 K^+ and 1372 Cl^-), was used in this study. In each run, an equilibrium state of the system was reached with a sufficiently long relaxation period for 2×10^4 steps (40 ps) under ambient conditions (0.1 MPa and 300 K). After this procedure, a further subsequent period of 3×10^4 steps (60 ps) was added, and we took the average of these data as the simulation results.

We performed MD simulations for a larger cell containing 1125 unit cells ($5 \times 15 \times 15$, 4500 K^+ and 4500 Cl^-) to investigate crystalline states. The van der Waals interactions were based on the polarization of molecules and the induced short ranged force. We changed the potential parameters to allow discussion of the effects of short ranged force affected by van der Waals interactions on the B1–B2 phase transitions.

2.2. Dislocation

As regards dislocations, a larger cell containing 10 620 atoms (5310 K^+ and 5310 Cl^-) was used. An MD cell with 1350 unit cells ($6 \times 15 \times 15$, 5400 K^+ and 5400 Cl^-) was produced; then the same number of potassium and chloride atoms (90 atoms each) along the a-axis direction were deleted to make a trench, maintaining 2×10^4 steps under ambient conditions (0.1 MPa and 300 K). The MD cell was set under 1 GPa for 2×10^4 steps (40 ps) to close the trench, and dislocations were successfully generated in the basic MD cell.

3. Results and discussion

3.1. Perfect crystal

Figure 2 shows the crystalline states in the process of the phase transition from a B1-type structure to a B2-type one (19 GPa and 300 K). Figure 2(a) shows the starting state of a

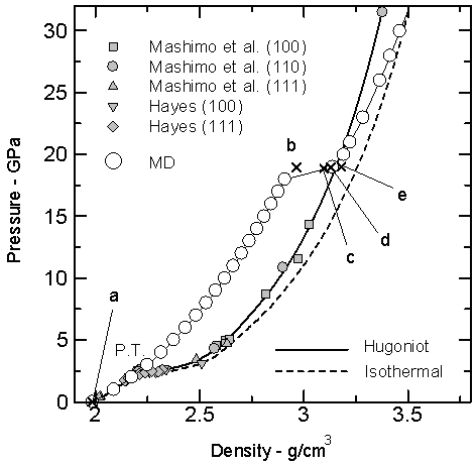

Figure 3. The Hugoniot compression curve, isothermal compression curve and MD simulation results. The alphabetical notation corresponds to that in figure 2.

B1-type perfect crystal projected in the ⟨100⟩ axis direction. Sufficiently long calculations under ambient conditions (0.1 MPa and 300 K) were performed for the initial relaxation. The density and the running K–Cl coordination number were 1.985 g cm^{-3} and 6.0, respectively; these are consistent with the experimental values for B1-type KCl. Figure 2(e) shows the resultant B2 phase after the phase transition (at 60 ps) under high pressure (19 GPa and 300 K) when viewed from a direction perpendicular to the page. The density and the running K–Cl coordination number became 3.180 g cm^{-3} and 7.66, respectively. The running K–Cl coordination number of 7.66 was close to the theoretical number for a B2-type structure of 8.0. The coordination number of 7.66, while not exactly consistent with the theoretical one of 8.0, indicated the presence of defects. In fact, the resultant B2 phase (figure 2(e)) included grain boundaries. In addition, the B1–B2 phase transition may be incomplete at 60 ps, because the phase transition occurs on a timescale much shorter than the experimental one. For these reasons the coordination number is not exactly consistent with the theoretical one. Figures 2(b)–(d) show the crystalline states in the phase transition process at 9.2, 10.0 and 10.4 ps, respectively. The MD simulation results for the EOS are plotted together with the Hugoniot compression curve and isothermal compression curve in figure 3. The states denoted by (a)–(e) in figure 3 correspond to those of figure 2. At 9.2 ps (figure 2(b)), the crystal structure was still a B1-type one. In addition, the crystalline state (b) in figure 3 was an extension of the B1 phase region of KCl. However, the atomic plane started to bend in the centre of the MD cell. At 10.0 ps (figure 2(c)), the phase transition proceeded, and the atomic planes bent too much, causing displaced atomic lines along the ⟨100⟩ axis direction of the B1-type structure, and increasing the density to 3.097 g cm^{-3}. The crystal structure was regarded as a B2-type structure, because the crystalline state (c) in figure 3 was in the B2 phase region. At 10.4 ps (figure 2(d)), the phase transition had almost finished except for the upper part of the basic MD cell, and the density became 3.129 g cm^{-3}. The simulation results indicated that the phase transition proceeded by the displacement of atomic lines along the ⟨100⟩ axis direction of the B1-type structure. These lines displaced, retaining their arrangement along the ⟨100⟩ axis direction of the B1-type structure, and as a result the B2 phase spread throughout. These lines are ascribed to the atomic lines along the ⟨111⟩ axis direction of a B2-type structure. This mechanism is different from Buerger's and the WTM mechanism,

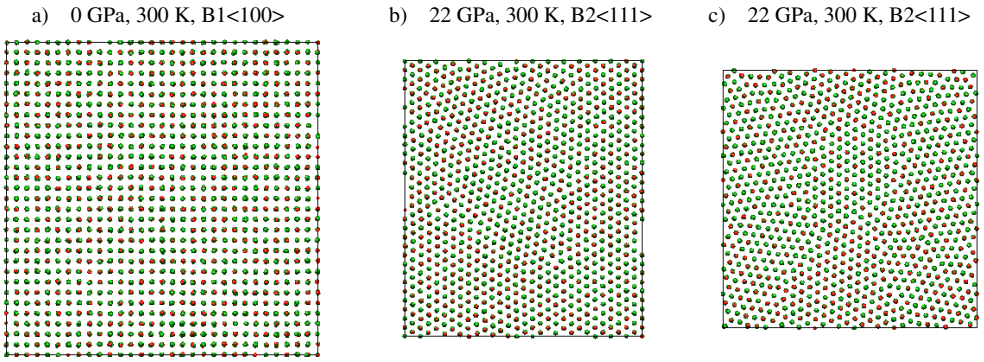

Figure 4. MD simulation results for a larger system with a perfect crystal (4500 K^+ and 4500 Cl^-). (b) and (c) were simulated under the same conditions (22 GPa, 300 K and 60 ps) except as regards potential parameters. (a) is the starting crystalline state of KCl, projected on the ⟨100⟩ axis direction of a B1-type structure. (b) is the resultant B2 phase with strong van der Waals interaction, and includes some dislocations. (c) is the resultant B2 phase with weaker van der Waals interaction than that of (b), and some clusters are generated.

which were previously proposed for alkali halides. In Buerger's mechanism, the B1–B2 phase transition was caused by atomic displacements along the ⟨111⟩ axis direction of the B1-type structure. In the WTM mechanism, the B1–B2 phase transition was explained in terms of displacements of the crystal layer of the B1-type structure, where the B2-type structure retained the orientation relations B1(011) ∥ B2(001) and B1(100) ∥ B2(110). In our results, the observed mechanism is different from both mechanisms. We propose that the B1–B2 phase transition is caused by displacements of atomic lines along the ⟨100⟩ axis direction of the B1-type structure and the orientation relation is found to be B1(100) ∥ B2(111).

The phase transition pressure obtained from MD simulations was significantly higher than the experimental data. This disagreement happens in MD simulation because the system has to surmount an energy barrier to transform from one phase to another, while thermodynamically the enthalpy of the new phase is already lower. The cell size effect is one of the reasons for the disagreement; however, increasing cell size will not make it exactly disappear even in the case of very large supercells. Therefore we calculated the thermodynamic phase transition points as follows: the phase stability was analysed using the difference in Gibbs free energy between the B1 and B2 phases of KCl. The Gibbs free energy was evaluated using the following equation:

$$\Delta G = \Delta E + P\Delta V = \Delta H \tag{2}$$

where Δ means the difference between the B1 phase and B2 phase. G, E, P, V and H are the Gibbs free energy, internal energy, pressure, volume and enthalpy, respectively. Some calculations for B1-type and B2-type perfect crystals were carried out. The G functions of the B1 and B2 phases were approximated as quadratic functions of pressure using the least squares method. The pressure at $\Delta G = 0$ shows the B1–B2 phase transition pressure in thermodynamics. The thermodynamic phase transition pressure was calculated to be about 3.5 GPa, which is very close to the experimental data (about 2 GPa).

Figure 4 shows the MD simulation results for a larger cell. Figure 4(a) was the starting crystalline state projected on the ⟨100⟩ axis direction of a B1-type structure, and containing 1125 unit cells ($5 \times 15 \times 15$, 4500 K^+ and 4500 Cl^-). Figures 4(b) and (c) show the resultant crystalline states of B2 phases (22 GPa and 300 K) with strong van der Waals interactions and weak ones, respectively. Viewed from a direction perpendicular to the page, the hexagonal-

like arrangement of atoms in figures 4(b) and (c) corresponded to the ⟨111⟩ plane of a B2-type structure. Similar to the case for the simulations for the smaller cell (1744 K^+ and 1744 Cl^-) in figure 2, a B2-type structure was formed. As a result, the atomic lines along the ⟨100⟩ axis direction of the B1-type structure corresponded to the ones along the ⟨111⟩ axis direction of a B2-type structure. However, in the case of the larger cell, the details of the phase transition behaviour were different from those for the smaller one. The phase transition partially occurred in the basic MD cell, and the B2 phase spread throughout (figures 4(b) and (c)). This was not so different from the process between figures 4(b) and (c), but the crystalline states of the resultant B2 phase were different. We changed the potential parameters of the van der Waals term to allow us to discuss the effects of short ranged force. van der Waals interactions are based on the polarization of molecules, which induce short ranged force. The simulation results for large and small parameters C_i and C_j are shown in figures 4(b) and (c), respectively. As the results show, some dislocations and clusters were generated in the B2 phase, as shown in figures 4(b) and (c), respectively. We assumed that the clusters of the B2 phase appeared when the short ranged force was weak; therefore, it is reported that the perfect crystal transformed to polycrystal under high pressure.

3.2. Dislocation

Figure 5 shows the process of the B1–B2 phase transition of KCl including dislocations. At the starting state, two pairs of two edge dislocations exist in a B1-type structure of KCl. A sufficiently long relaxation period (40 ps) was set under 1 GPa to make the dislocations, and these two edge dislocations crossed at right angles, as shown in figure 5(a). In the case of ionic crystals, anions and cations have to be next to each other. Two edge dislocations were generated, because there were not sufficient anions and cations around an edge dislocation in ionic crystals for them to be next to each other. At 4.4 ps (figure 5(b)), the B2 phase appeared around the dislocations and progressed to the arrows. Figure 5(c) (at 60 ps) shows the resultant crystalline state of the B2 phase projected on the ⟨111⟩ axis direction. The B1–B2 phase transition occurred at 12 GPa, which was lower than the phase transition pressure of the smaller cells. Similarly to the case for simulations without dislocations, the phase transition proceeded by the displacement of atomic lines parallel to the ⟨100⟩ axis direction of the B1-type structure. In addition, as the results show, atomic lines along the ⟨100⟩ axis direction of the B1-type structure corresponded to the ones along the ⟨111⟩ axis direction of the B2-type structure. The resultant crystalline state contained a grain boundary, as shown in figure 5(d), which was rotated by 39.4° around the *c*-axis direction.

4. Conclusions

We performed MD simulations to investigate the process and the effects of defects on the B1–B2 phase transition of the ionic crystal KCl. We adopted the Born–Mayer–Huggins-type potential function as the interatomic interaction, and the potential parameters were empirically determined using lattice parameters and bulk moduli on the basis of the Hugoniot EOS data by fitting them to the Birch–Murnaghan equation of state. A larger cell with no defects, containing 9000 atoms (4500 K^+ and 4500 Cl^-), was employed as a basis for discussing the kinetics of the phase transition and the crystalline states. MD calculations for dislocations were also carried out for investigating the effects of defects in the ionic crystal KCl under high pressure.

The simulation results showed that the B1-type structure of a KCl perfect crystal transformed to a B2-type structure under hydrostatic high pressure, and that it showed a reversible transition with large hysteresis. From the results of thermodynamic analysis,

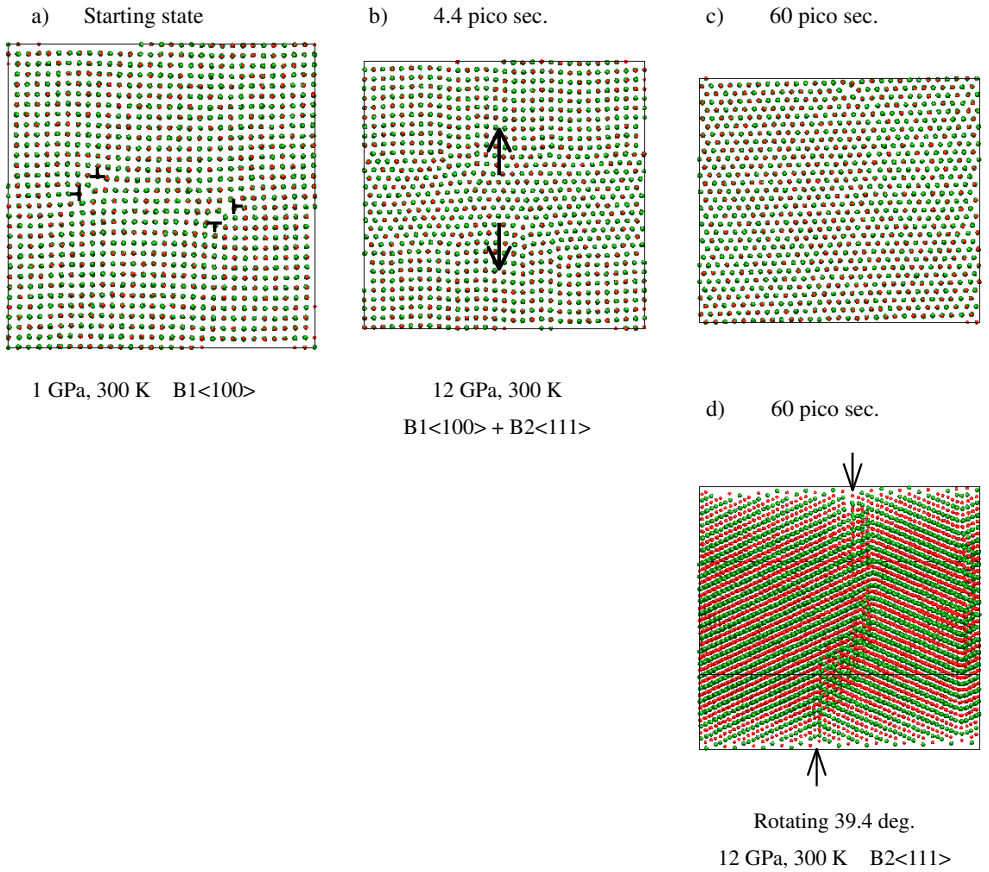

Figure 5. The process of the B1–B2 phase transition of KCl with dislocations. (a) is the starting crystalline state of KCl, projected on the ⟨100⟩ axis direction of a B1-type structure. It has two pairs of edge dislocations under 1 GPa. In (b), the B2 phase expands to the arrows, and spreads throughout. (c) is the resultant B2 phase with a grain boundary, and (d) is rotated by 39.4°, and the boundary is observed between the arrows.

the thermodynamic phase transition pressure was calculated to be 3.5 GPa. The simulation results indicated that the phase transition proceeded by the displacement of atomic lines along the ⟨100⟩ axis direction of a B1-type structure; and as the results show, the atomic lines corresponded to the ones along the ⟨111⟩ axis direction of a B2-type structure. This observed mechanism is different from others proposed previously. The simulation results for the large scale calculations showed that some dislocations or clusters were generated in the resultant B2 phase; these were simulated using strong and weak van der Waals interactions, respectively. As regards dislocations, the phase transition started around the dislocations and the phase transition pressure decreased to 12 GPa.

We intend to investigate phase transitions for other alkali halides as a basis for discussing crystalline states under static and shock compressions, and for other extreme conditions.

Acknowledgment

This work was supported in part by the 21st century COE programme on Pulsed Power Science in Kumamoto University.

References

[1] Bridgman P W 1945 *Proc. Am. Acad. Arts Sci.* **76** 1
[2] Bassett W A, Takahashi T and Campbell J K 1969 *Trans. Am. Cryst. Assoc.* **5** 93
[3] Nagasaki H and Minomura S 1964 *J. Phys. Soc. Japan* **19** 1496
[4] Vaidya S N and Kennedy G C 1970 *J. Phys. Chem. Solids* **32** 951
[5] Kusaba K and Syono Y 1993 *Rigaku-Denki J.* **24** 18
[6] Yagi T 1977 *J. Phys. Chem. Solids* **39** 563
[7] Hayes D B 1974 *J. Appl. Phys.* **45** 1208
[8] Dremin A N, Pershin S V and Pogorelov V F 1965 *Combust. Explos. Shock Waves* **1** 1
[9] Mashimo T, Nakamura K, Tsumoto K, Zhang Y, Ando S and Tonda H 2002 *J. Phys.: Condens. Matter* **14** 10783
[10] Devani S and Anwar J 1996 *J. Chem. Phys.* **105** 3215
[11] Parrinello M and Pahman A 1981 *J. Phys. C: Solid State Phys.* **6** 511
[12] Buerger J 1951 *Phase Transformation in Solids* ed R Smoluchowski, J E Mayer and W A Weyl (New York: Wiley)
[13] Ruff I, Baranyai A, Spohr E and Heinzinger K 1989 *J. Chem. Phys.* **91** 3148
[14] Watanabe M, Tokonami M and Morimoto N 1977 *Acta Crystallogr.* A **33** 294
[15] Recio J M, Martin Pendas A, Francisco E, Florez M and Luana V 1993 *Phys. Rev.* B **48** 5891
[16] Kawamura K 1996 Japan Chemistry Program Exchange (JCPE)
[17] Ewald P 1921 *Ann. Phys.* **64** 253